applied sciences

MDPI

Article

Evaluating V2X-Based Vehicle Control under Unreliable Network Conditions, Focusing on Safety Risk

Roland Nagy [1,2], Árpád Török [1,*] and Zsombor Pethő [1]

[1] Faculty of Transportation Engineering and Vehicle Engineering, Department of Automotive Technologies, Budapest University of Technology and Economics, 1111 Budapest, Hungary; nagyr@edu.bme.hu (R.N.); petho.zsombor@kjk.bme.hu (Z.P.)
[2] Jaguar Land Rover Hungary Ltd. Organization, 1134 Budapest, Hungary
* Correspondence: torok.arpad@kjk.bme.hu

Abstract: With the emergence of Vehicle-to-Everything (V2X) systems, it is important to investigate how deteriorating network parameters affect vehicle functionality based on wireless communication. It is important to determine how we can prevent the performance degradation of these functions and ensure safety on the roads. This paper examines the potential for enhancing the performance of a connected vehicle function by considering network parameters in the control algorithm. In order to achieve this, a safety indicator was incorporated into the control algorithm, which takes into account both vehicle dynamics and network parameters. Following an assessment of the proposed control method, it was determined that it is a suitable approach for enhancing the performance of the vehicle function.

Keywords: V2X; noise; CACC; network performance; safety risk; PDR

Citation: Nagy, R.; Török, Á.; Pethő, Z. Evaluating V2X-Based Vehicle Control under Unreliable Network Conditions, Focusing on Safety Risk. *Appl. Sci.* **2024**, *14*, 5661. https://doi.org/10.3390/app14135661

Academic Editors: Ryan Cheuk Pong Wong, Jintao Ke and Fangni Zhang

Received: 24 May 2024
Revised: 22 June 2024
Accepted: 26 June 2024
Published: 28 June 2024

1. Introduction

In the near future, we will experience a new era in the vehicle and transportation industries as the development of new technologies gets to a new level. Autonomous driving has been a long-awaited improvement that could improve the safety and efficiency of our transport system. To enable autonomous features and vehicles, a new way of perception and communication had to be introduced to the industry in the form of Vehicle-to-Everything (V2X) communication. With this development, vehicles could send static and dynamic information about themselves to nearby system components. With the acquired data, vehicles will be able to create a local dynamic map (LDM) to improve ad hoc decision making and the safety of transportation. Moreover, with over-the-air communication between vehicles, previously unpredictable scenarios, like non-line-of-sight (NLOS) scenarios, can become safer, while line-of-sight (LOS) scenarios also benefit from the additional redundancy against sensor malfunction. To achieve this, two separate ways of communication are in development. One of them is Dedicated Short-Range Communication (DSRC), which is based on the IEEE 802.11p standard [1]. The alternative is Cellular-V2X (C-V2X), which was widely promoted by the 3GPP organization. Cellular networks are expected to improve vehicular communications as simulation research shows that C-V2X outperforms DSRC in terms of communication range. DSRC is considered to operate up to a maximum of 1000 m, while C-V2X could have a coverage of up to several kilometers away [2–4]. A study performed by Petrov et al. [5] benchmarked DSRC and LTE-based C-V2X technologies. Based on their study, DSRC was able to achieve an average end-to-end latency of less than 100 milliseconds and an adequate packet delivery ratio (PDR) in all of the scenarios they investigated. In [6], the authors performed an exhaustive evaluation of available wireless technologies between vehicles in highway scenarios. Based on their evaluation, C-V2X, in general, has a higher operating range, but DSRC communication offers lower latency in low-density scenarios. In [7], the authors compared the performances of DSRC and

LTE-V2X under urban scenarios. Meanwhile, DSRC is dedicated to Cooperative Intelligent Transportation Systems (C-ITSs), until LTE-V2X shares a network with other LTE applications (such as video streaming and VoIP). This aspect negatively influences LTE-V2X, and their results showed that DSRC outperforms LTE-V2X.

Despite the intensive evolution of these new technologies, there are still a few gaps that need to be filled before they could be used in safety-critical automotive applications. One issue is the availability of the necessary information in specific high-risk situations. In safety-related applications, such as accident prevention or platooning, the timely arrival of messages from other vehicles or roadside units (RSUs) is crucial [8]. In degraded networks, where the quality of service (QoS) parameters are not adequate, the industry will have to focus on developing different control solutions to handle these conditions safely.

Aiming for this research gap, we started to review relevant studies related to V2X technologies. Knowle et al. [9] studied Vehicle-to-Vehicle (V2V) communication performance and its impact on safety distance. They were able to prove the importance of a reliable communication in achieving a shorter stopping distance and reducing reaction time. Schmidt et al. [10] studied the degradation of a vehicular ad hoc network (VANET) and found that the reliability of the network is a key requirement for V2V communication. Their simulation highlighted that transmission distance can be severely reduced. Their work was evaluated based on a traffic jam scenario where the vehicle density was high and the network degradation was caused by the other vehicles' interference. Consequently, their work showed that, in degraded network conditions, the available reaction time is shortened due to a lack of information. A study conducted by Hoque et al. [11] investigated the impact of On-Board Unit (OBU) placement, relative velocity, and relative altitude on V2X communication. They found OBU placement to have a significant impact because the transmission distance is greatly reduced when messages have to go through different obstacles inside the vehicle. A higher relative velocity results in decreased time when transmission can happen. In the case of altitude, based on their study, it could also provide a constraint to DSRC communication in terms of transmission distance. Choi et al. [12] researched a congestion control scheme that takes into consideration the QoS parameters. In their paper, they focused on the vehicle density effect on their two proposed models. In the first model, they wanted to keep the update rate at the cost of a reduced range, and in the other, they wanted to protect the range at the cost of the update rate. The results showed that V2X applications can be given a degree of freedom in choosing the QoS model. Park et al. [13] investigated the interferences' effect on DSRC-based communication. They proposed an interference-rejecting scheme, considering vehicle speed, Signal-to-Interference and Noise (SINR), and other channel conditions. This method resulted in a higher SINR performance in both low- and high-velocity cases. In a research conducted by Ali et al. [14], they studied the network-level and application-level reliabilities in connected vehicular networks. They investigated different path-loss models in a moderate transmission distance. To be able to mitigate the signal attenuation effect, they proposed a feedbackless relay method, which selects the farthest vehicle as a relay vehicle and rebroadcasts the message. This method is able to increase the network- and application-level reliabilities.

Cooperative driving is a promising way to improve traffic safety, but an unreliable network could lead to severe harm. Thunberg et al. [15] researched this topic, especially focusing on the age of information. They proposed a solution called safety time function to provide the duration available for a vehicle to react even in dense traffic situations. Liu et al. [16] studied the cooperative adaptive cruise control (CACC) as an advanced function for vehicle platooning that heavily relies on network performance. They proposed a control solution for fatal wireless communication failure. They assumed that, in degraded network conditions, the CACC transitions only to an sensor-based ACC. They proposed a solution during the transition phase to decrease jerk and thereby improve safety.

2. Motivation and Contribution

In this study, we developed a control concept that could mitigate the risk of accidents in case of a degraded or noisy environment. We chose to utilize DSRC communication for our CACC function. The rationale behind the selection of DSRC was that the majority of vehicles currently available on the market that are equipped with V2X capabilities utilize DSRC technology, which renders this a pertinent subject for testing [17]. We created a simulation environment where we can simulate the physical layer of the transmission and we are able to degrade the network performance by manipulating the Signal-to-Noise Ratio (SNR). We compared the proposed control algorithm with a simple CACC and evaluated how the different modulations affect the performance of the system and how the newly developed control concept can respond to the revealed problems.

Clearly, there is a significant potential to improve safety through the increased automation of transport systems. Automatic intervention in various vehicle systems is made possible by the widespread use of sensors that detect objects in the environment. This characteristic of highly automated systems provides an opportunity to reduce the likelihood of human error and the severity of any errors that do occur. It should be noted, however, that because they are highly dependent on environmental conditions, even modern sensor systems are severely limited in their applicability. With regard to camera or lidar systems, a non-line-of-sight (NLOS) scenario can occur, e.g., in a densely built-up urban environment or in heavy fog. In such cases, V2X can be used as a 360° sensing system to help make a safe decision [18]. However, the problem can be exacerbated if an NLOS scenario also occurs for radio communications [19]. In these cases, it is essential that the system makes decisions regarding vehicle control, taking into account risk factors like communication delay, packet loss, and speed.

With these considerations in mind, this paper presents a concept capable of making vehicle control decisions in NLOS situations of radio-based vehicle functions, taking into account risk factors that affect the safety of the system. The proof of concept presented here is not intended to work as a final control solution that can be applied industrially, but primarily to demonstrate the applicability of the method and the validity of the considerations introduced. These objectives have been achieved through the simulation of the selected scenarios. Investigating the safety implications of the method has provided convincing results.

3. Methodology

In our research, we used Matlab Simulink 2023b to create the simulation environment for a DSRC-based V2X system. We created the network's physical layer based on the IEEE 802.11p standard; however, we emphasize that the introduced general concept can be flexibly adapted to cellular technology-based systems. The following subsections will present the proposed control concept, the simulation environment, and the performed scenarios.

3.1. Safety Risk-Based Cooperative Adaptive Cruise Control (SRI-Based CACC)

In the context of our control concept (see Figure 1), the CACC is responsible for calculating the acceleration required to achieve the reference speed. The reference speed can be set by the driver or in the event that the actual risk is deemed to be too high, updated by the system. The CACC function is based on a standard MPC controller, and it considers the relative velocity, the relative distance, and the HV velocity as input variables. The Safety Risk Index (SRI) block is responsible for resolving the optimization problem of minimizing the difference between the tolerable and actual risk by manipulating the value of the reference speed. Our proposed control could overwrite the reference speed set by the driver if the mentioned SRI is higher than the predefined target value.

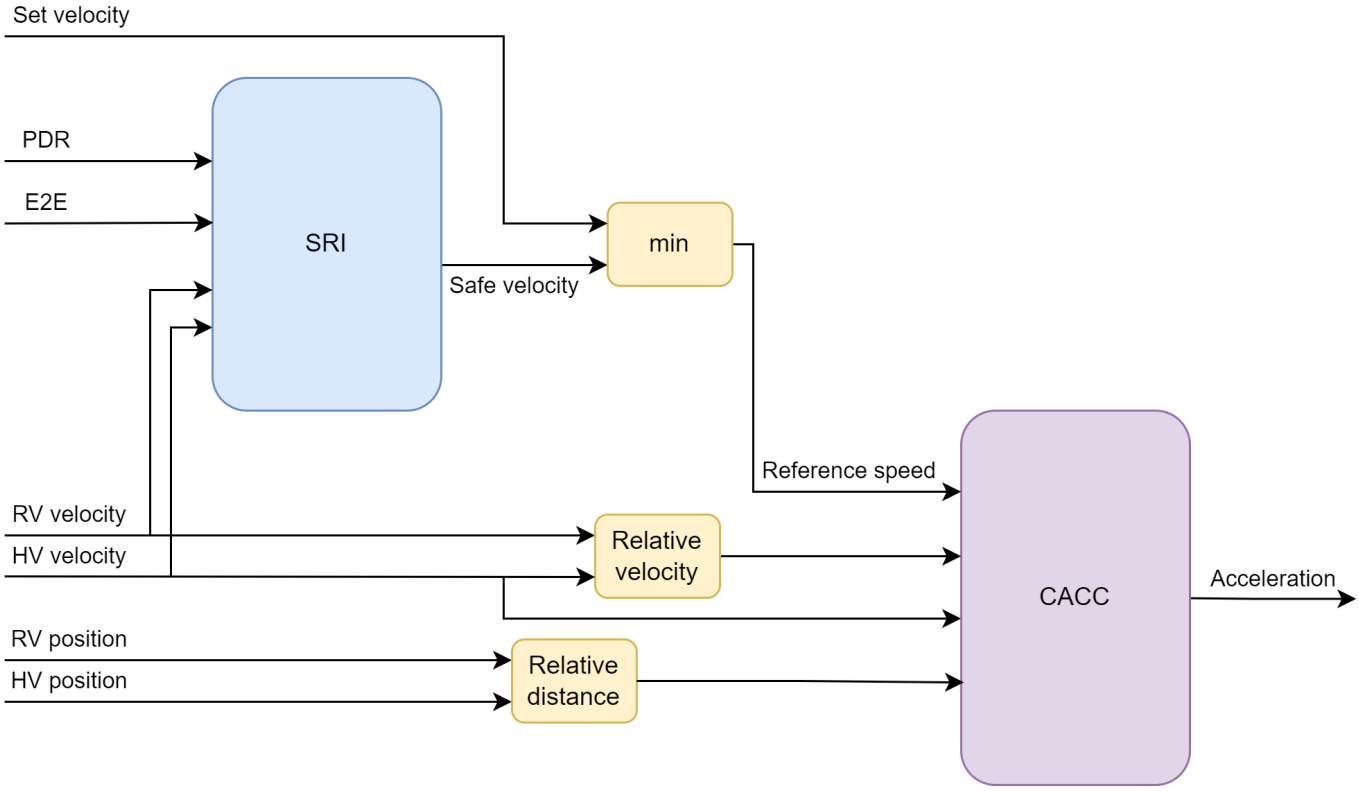

Figure 1. Control algorithm.

To be able to react to changes in network performance, we have to propose a new control structure that takes into consideration the QoS parameters, like PDR and end-to-end latency (E2E). In this research, we adopted the risk estimation function (1) proposed by Petho et al. [20] to quantify the safety risk of a particular traffic scenario.

$$SRI = f(v_{HV}, v_{RV}, PDR, E2E) \tag{1}$$

We modified the CACC reference speed calculation algorithm to take into consideration the Safety Risk Index (SRI). For calculating SRI, we used host vehicle (HV) and remote vehicle (RV) velocities and the PDR and E2E values.

When determining the network performance metrics, we only considered the PDR value, as our previous experience suggests that latency has a much less negative impact on safety risk. Accordingly, latency is assumed to be ideal, so E2E is set to zero. Furthermore, as an important extension of the previous concept, the network monitoring module cannot determine the PDR until the first packets are received, so it predicts with the ideal value of 100%. After the first successful reception, the network monitoring module starts to calculate the PDR as a last second mean value, which is a sliding window method-based aggregation. In order to improve the applicability of the method, we have defined a sufficiently low target for SRI in order to prevent a too aggressive intervention in low-risk scenarios. If we surpass this target, then the proposed function limits the host vehicle's velocity to meet these predefined criteria, thereby improving safety. Additionally, we have defined further constraints for the minimum safe velocity calculation. In the case of the newly introduced method, we set 10 m/s as an absolute minimum value. If the vehicle receives a correct packet with a valid velocity value higher than the absolute minimum, then this is used as the minimum value for the a velocity calculation.

3.2. Simulation Environment

Our simulation environment could be separated into five modules as in Figure 2. The first one is the vehicle dynamic module, which is a six-dimensions-of-freedom (6-DOF)

electric vehicle model that has one engine on the rear axle. This complex model was chosen to support a realistic vehicle simulation and reliable conclusions. The second module contains the vehicle control function, while the third module is responsible for the scenario initialization and actor control.

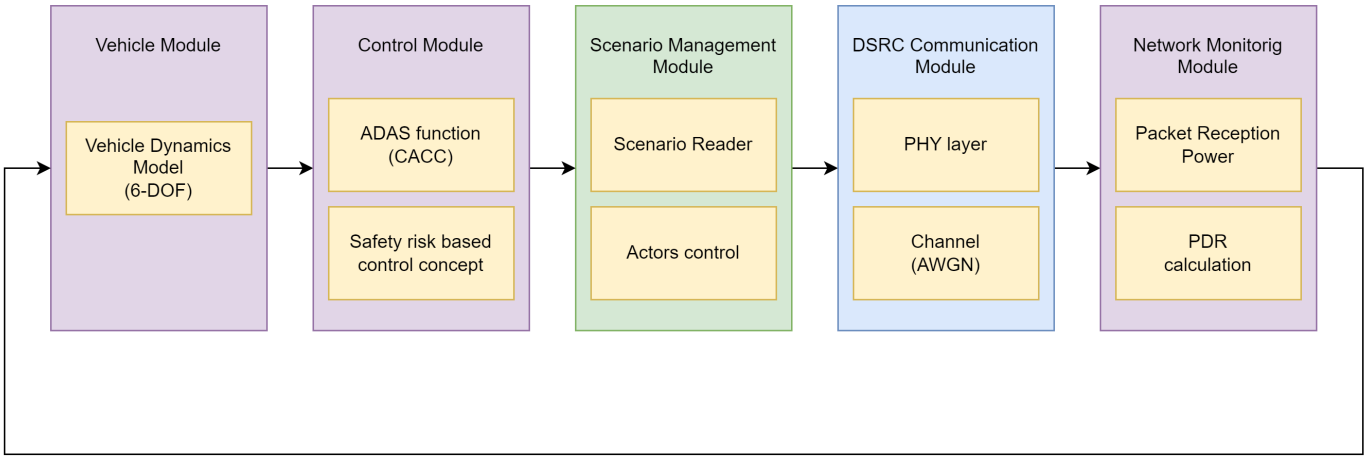

Figure 2. Simulation environment.

The fourth module implements the DSRC network physical layer and the data transmission between vehicles. In this module, we can perform the network degradation by manipulating the additional noise for our simulation. In the last module, we have implemented a simple network monitoring algorithm to be able to check the network state throughout the simulation. As a major contribution of our research, we have developed a new control concept to deal with the uncertainty caused by the degraded communication and to reduce the risk posed by wireless communication. This includes the use of the introduced SRI function, which allows the system to respond to changes in network quality.

3.3. Communication Model

This section serves as one of the core areas of our research, aimed at facilitating wireless communication between vehicles. For the simulation, we created a basic message frame that contains the most relevant parameters, including global positions, velocities, angular velocities, and the roll, pitch, and yaw values. Additionally, the created frame starts with the actor ID and timestamp with three additional spaces for other parameters at the end of the message structure. These 18 parameters are converted to 16-bit integers. With regard to bit size, this corresponds to the size of a basic container field in a Cooperative Awareness Message (CAM), where these vehicle parameters are stored [21]. In the initial stages of our investigation, it is essential to determine the methodology for computing and adjusting the SNR value. Throughout the simulation, we maintained the transmission power (P_T) at a constant value of 23 dBm, a standard setting for DSRC communication. As one of the objectives of this investigation is to assess the impact of packet loss on a proposed control, it is essential to determine the receiving power (P_R) in accordance with Equation (2).

$$P_R = P_T - FSPL - X_\sigma \tag{2}$$

$$FSPL = 10 \cdot log_{10}\left(\frac{4 \cdot \pi \cdot d \cdot f_c}{c}\right)^2 \tag{3}$$

The free space path loss (FSPL) is a simplified method for simulating the message power attenuation between the transmitting and receiving sides. In Equation (3), we consider the distance between two antennas (d), the carrier frequency (f_c), and the speed of light (c). In this research, we employed the single-slope model. According to other measurements, the difference in a double-slope model was minor [22]. Shadowing (X_σ) uses a log-normal random distribution with a mean value of zero. For our research, we

used 3.7 dB for a standard deviation based on [22]. Once we determined the receiving power, we can calculate the SNR of the communication (see Equation (4)).

$$SNR = P_R - N_0 \tag{4}$$

$$N_0 = N_{thermal} + N_{other} \tag{5}$$

The performance of background noise (N_0) can be affected by a number of factors, including ambient noise and radio frequency interference. In the present simulation, thermal noise was employed as the principal noise source, and its value was calculated according to Equation (6).

$$N_{thermal}\ [\text{dB}] = 10 \cdot log_{10}(1000 \cdot B \cdot T \cdot k) \tag{6}$$

For our simulation, we considered the 10 MHz bandwidth (B), which is dedicated to DSRC communication, and an ideal temperature of 297 K (T). The last element of Equation (6) is the Boltzmann constant (k). This allows us to calculate the SNR value by subtracting the noise from the received power. In our study, we wanted to simulate a degraded network, which we were able to perform with a varying SNR value. For this, we considered additional noise (N_{other}) values that would establish a degraded network (Equation (5)).

In the second stage of the process, the created message must undergo a complex series of transformations before reaching the host vehicle (HV). Our approach was to follow the IEEE 802.11p standard to set up the physical layer of DSRC communication in Simulink, as shown in Figure 3.

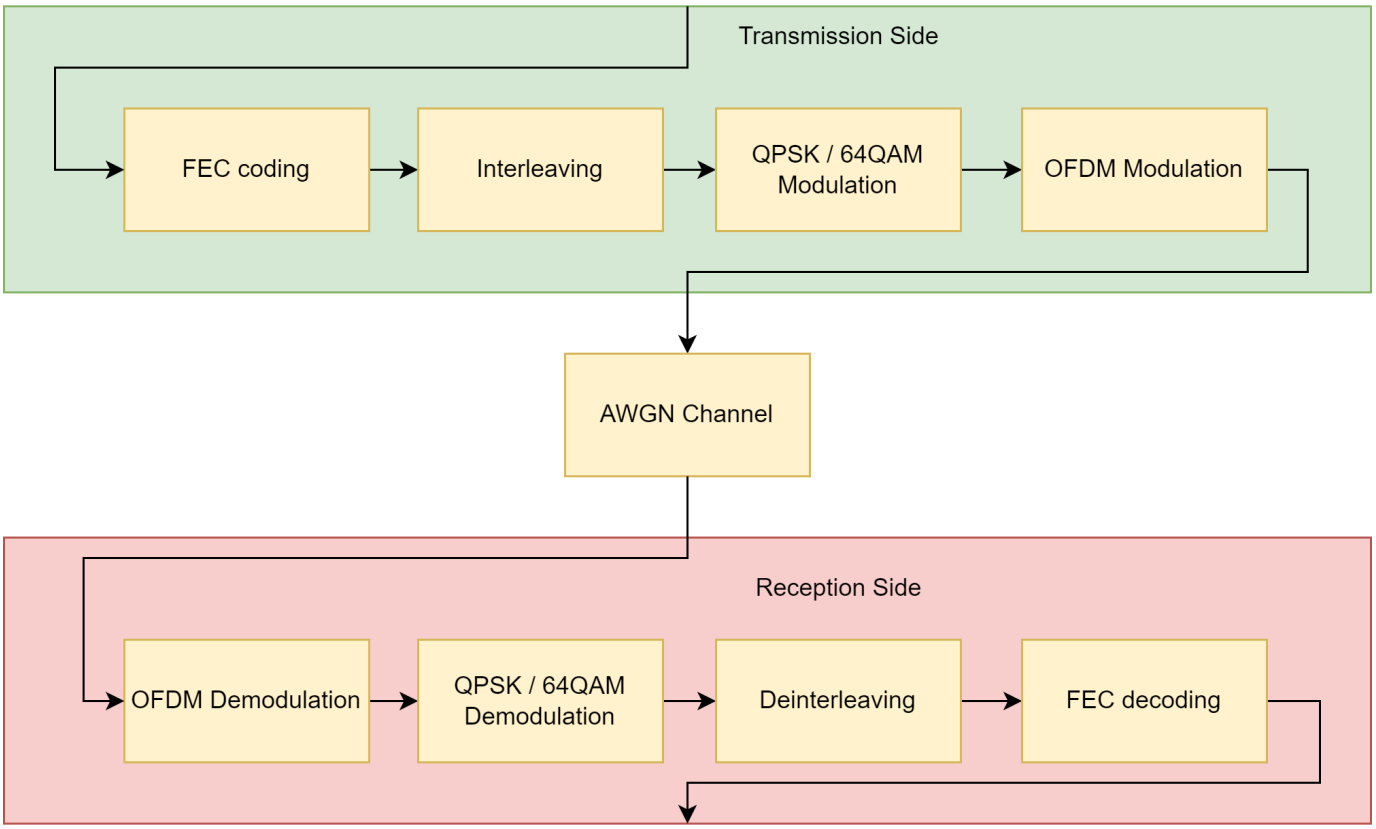

Figure 3. Bit stream way throughout the physical layer.

Once the required data have been converted into bits, forward error correction (FEC) is applied to the bit stream, depending on the selected modulation. In our work, we have selected four standard modulations [23] in order to investigate the effect of different

modulations on the proposed control performance. These modulations can be seen in Table 1 with their working conditions.

Table 1. Different modulations.

Mode	Coding Rate and Modulation	Receiver Sensitivity [dB]	LoS Range [m]
1	1/2 QPSK	−82	541
2	3/4 QPSK	−80	439
3	2/3 64QAM	−69	139
4	3/4 64QAM	−68	125

After FEC coding, interleaving is used to prevent the occurrence of long sequences of adjacent noisy bits. The required modulation is then applied to the bit stream before it is transmitted to the channel. The Orthogonal Frequency Division Multiplexing (OFDM) modulation is applied last, before transmission. To simulate the effect of ambient noise on the message, we introduced additive white Gaussian noise (AWGN) into the channel. As specified in the 802.11p standard [24], the standard parameters for OFDM modulation were used (see Table 2).

Table 2. OFDM modulation parameters.

Data Subcarriers	FFT Length	Guard Bands (Left–Right Side)	DC Null	Pilot Subcarriers (Positions)	Cyclic Prefix	OFDM Symbol
48	64	5–6	yes	4 (12, 26, 40, 54)	16	6 (QPSK), 2 (64QAM)

In contrast to the encoding process, the decoding is initiated by the receiving device in reverse as it was on the transmitting side. In the initial phase, the receiving device assesses the message reception power. If this is below the receiving sensitivity of the modulation threshold, then the module assumes that the message has not been received. Conversely, if the reception power is above the sensitivity threshold, the device attempts to decode the message. Decoding is a crucial aspect of this layer, as it enables the recipient to obtain the information they require from the sender.

3.4. Scenarios

In order to demonstrate the results of our research, it was necessary to investigate a number of scenarios in which our proposed concept could be tested. We selected and created a typical line-of-sight (LOS) scenario in which we altered the velocity difference between the host and the remote vehicle (see in Table 3).

Table 3. Three scenarios with constant velocities (Host Vehicle (HV), Remote Vehicle (RV)).

HV Target Velocity [m/s]	RV Velocity [m/s]	Starting Inter-Vehicular Distance [m]	Additional Noise [dB]
25	16.67	200	20 at 400 m
25	11.11	200	20 at 400 m
25	2.78	200	20 at 400 m

In addition, as part of the investigation of the control mechanism to mitigate the effects of a degraded network performance, a simple noise generator was introduced at a distance of 400 m from the HV starting position. This additional interference generator has been included to make the scenario more complex for the V2X communication and to facilitate the testing of our proposed control concept in a noisy environment. As illustrated in Figure 4, the noise generator covers an area with a 400 m radius, with a 20 dB signal strength at the center point, which then gradually decreases as we move away from the source.

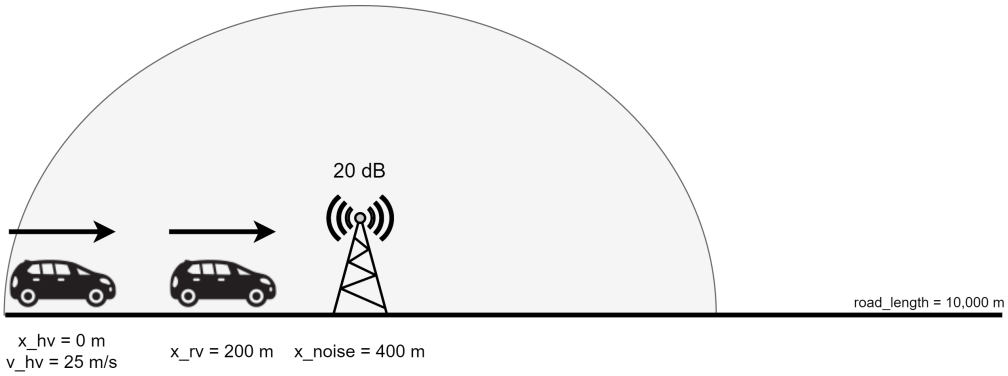

Figure 4. Implemented scenario description.

4. Results and Discussion

In this section of the paper, we present and evaluate the results of our simulations. We investigated three distinct scenarios, each with and without the safety risk-based (SRI) control concept. In each case, we initiated the HV with an initial velocity of 20 m/s, aiming to accelerate it to 25 m/s with the CACC. The default values for the control algorithm included a 300 m relative distance when there was no vehicle in front of the host vehicle and a 100% probability of PDR until the appropriate message could be decoded by the V2X module. If the appropriate message was received, the packet was stored until a new message was received. The perception module used the last correct value until a newer one arrived, so if the host vehicle perceives the remote vehicle and it is no longer in front, it will use the previously mentioned 300 m as a default value. In this simulation, the effect of latencies on the controller has not been considered, as this aspect will be addressed in the future development of the simulation environment.

4.1. Low Relative Velocity Scenario

First, we initiated our simulation with a more common scenario where the two vehicles' delta velocity was low. Figure 5 illustrates the results obtained when we employed the default CACC without any additional control method. As the figure shows, the four different modulation schemes exhibited a comparable performance, with the 64QAM modulation exhibiting a slight discrepancy. This is due to the fact that this modulation is more complex, resulting in a reduced operational distance. The discrepancy can be observed in the relative distance plots as the two vehicles enter the noisy environment. For the QPSK modulation with both coding rates, the packets still arrived, although a few were lost in the vicinity of the maximum noise level. In comparison, the 64QAM modulation was unable to maintain a robust connection in the presence of noise, necessitating the use of the last known position of the target vehicle as a reference point for the perception module.

Consequently, the relative distance gradually decreases until it reaches zero, which represents the point of potential collision. However, at this point, the value is not accurate, and the vehicle responds with a delay before accelerating to reach the desired speed. Once the HV has departed from the noisy environment, it receives the most recent information and begins to adjust its velocity to align with the remote vehicle's velocity. In the middle plot, we show SRI throughout the simulation, but the control mechanism is deactivated. The high value can be attributed to the low PDR values.

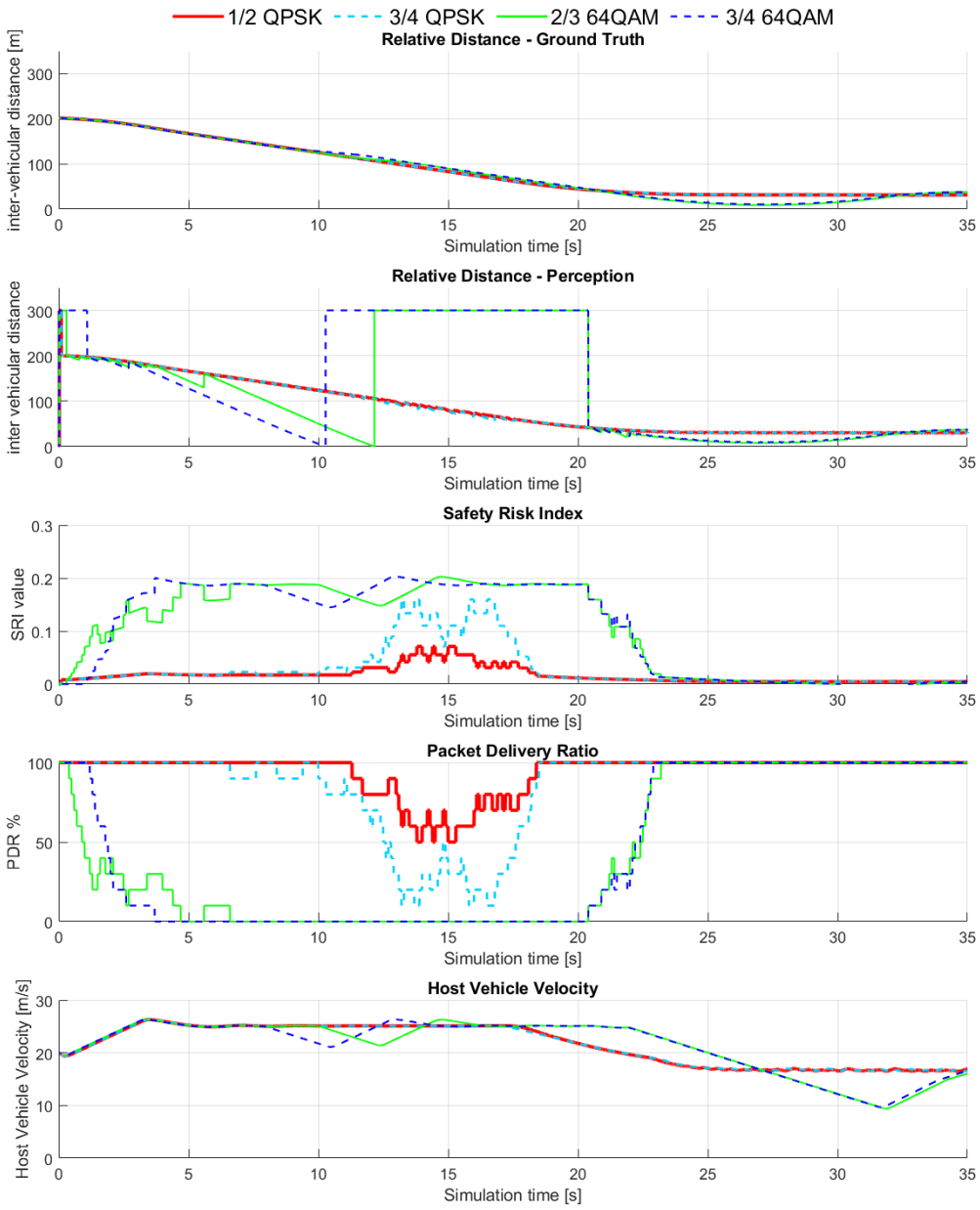

Figure 5. Results from simple CACC for low relative velocity (8.33 m/s = 30 km/h).

In Figure 6, we conducted a similar experiment with our proposed control concept. On the fourth plot, we can observe PDR values similar to those in a simple CACC method. The SRI values were slightly lower than those without the suggested control due to the control's impact on the delta velocity between the two vehicles. In the case of QPSK, the change in relative distance was comparable to that in the simple method, but our method was slightly more cautious. Upon evaluating the 64QAM modulation, it became evident that the SRI values exceeded the desired threshold as soon as the network experienced degradation. Consequently, the control reduced the velocity. Based on the last received message, it appears that the perceived relative distance values are falsely represented. However, when the ground truth is considered, it becomes apparent that the control is almost overly cautious, and the two vehicles are situated at a considerable distance.

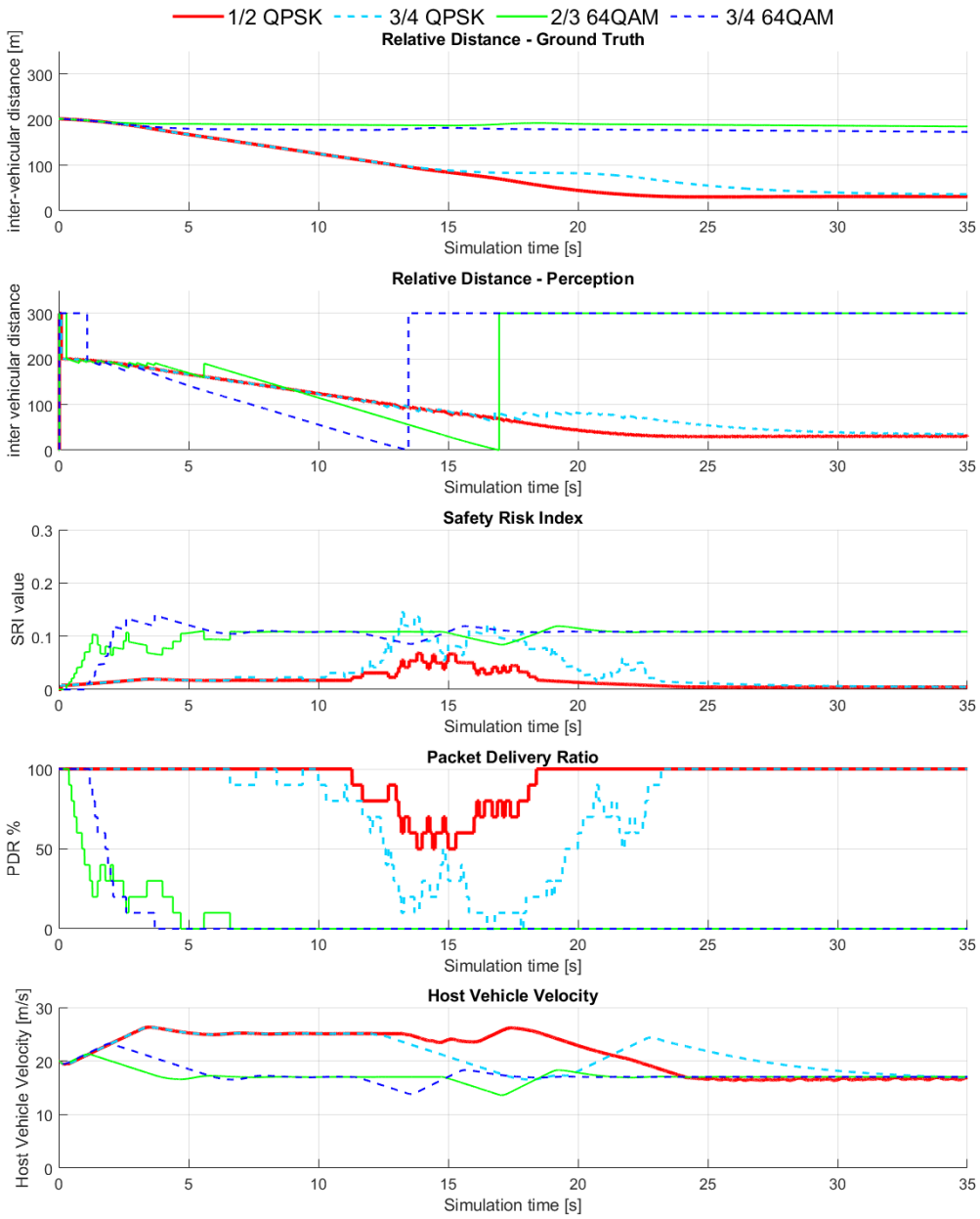

Figure 6. Results from SRI-based CACC for low relative velocity (8.33 m/s = 30 km/h).

4.2. Moderate Relative Velocity Scenario

To test our concept more deeply, we increased the delta velocity between the vehicles to 50 kph. In Figure 7, the simple CACC was evaluated in multiple plots. From the relative distances and HV velocity plots, it can be seen that almost all of the modulations were able to adapt to the remote vehicle velocity and keep a safe distance between them. In the case of 64QAM modulations, the PDR dropped to very low values, and the 3/4 coding rate was unable to react in time. At approximately the 18th second of the simulation, a collision occurred between the two vehicles.

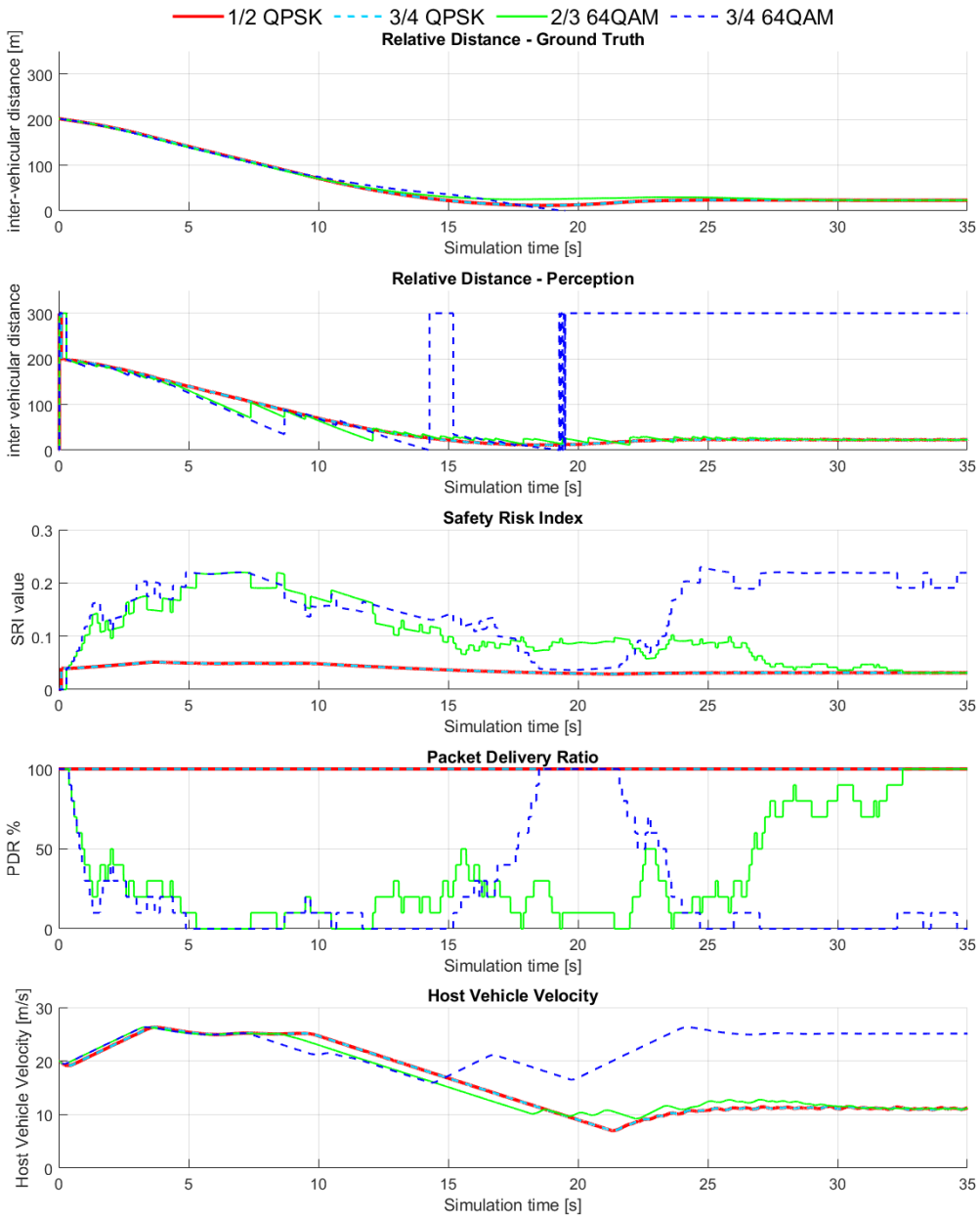

Figure 7. Results from simple CACC for moderate relative velocity (13.89 m/s = 50 km/h).

The QPSK modulations exhibited resilience to the noisy environment, likely due to the higher velocities.

An analysis of the proposed control in Figure 8 reveals that a similar outcome occurs with the QPSK modulation. The network quality remains almost perfect throughout the simulation, even in a noisy environment. However, when we examine the 64QAM modulation, we observe a decline in network performance when an additional interference occurs. As a result of the deteriorated network, SRI begins to rise, prompting the HV to decelerate in order to reduce the probability of a collision. From a relative distance, it can be inferred that our control is excessively cautious in this instance, yet there were no incidents in any of the aforementioned scenarios.

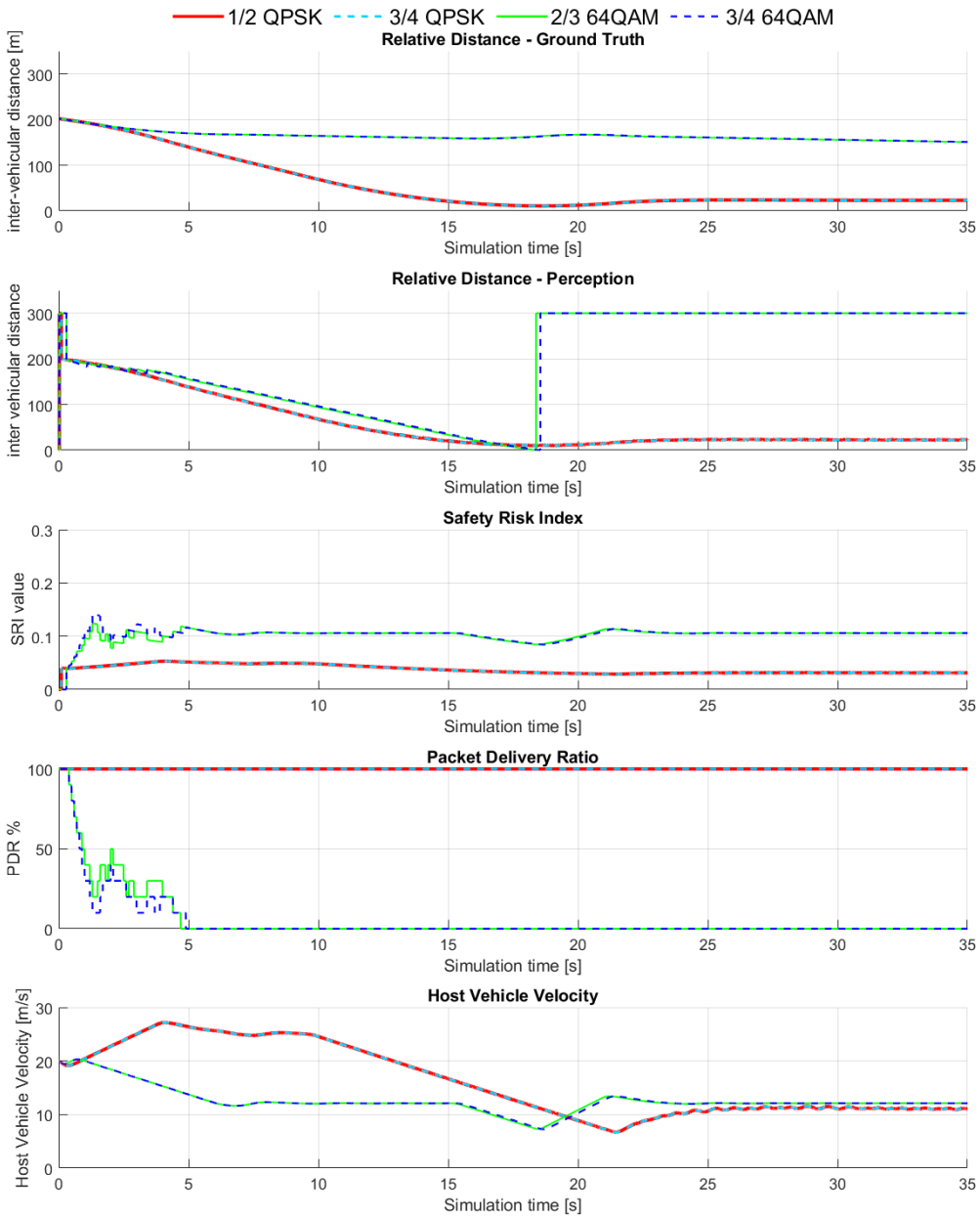

Figure 8. Results from SRI-based CACC for moderate relative velocity (13.89 m/s = 50 km/h).

4.3. High Relative Velocity Scenario

Finally, we investigated a scenario in which the remote vehicle slows down suddenly due to an unforeseen event on the road. Due to the high delta velocity, none of the modulation techniques were able to react in time to prevent the accident, as illustrated in Figure 9. SRI was high from the beginning of the simulation due to the high velocity differences and, in the case of the 64QAM modulation, the network degradation. Following the collision, which occurred approximately 11 s into the simulation, the presented plots are no longer valid. However, this illustrates that even the QPSK modulation was no longer within the reception distance.

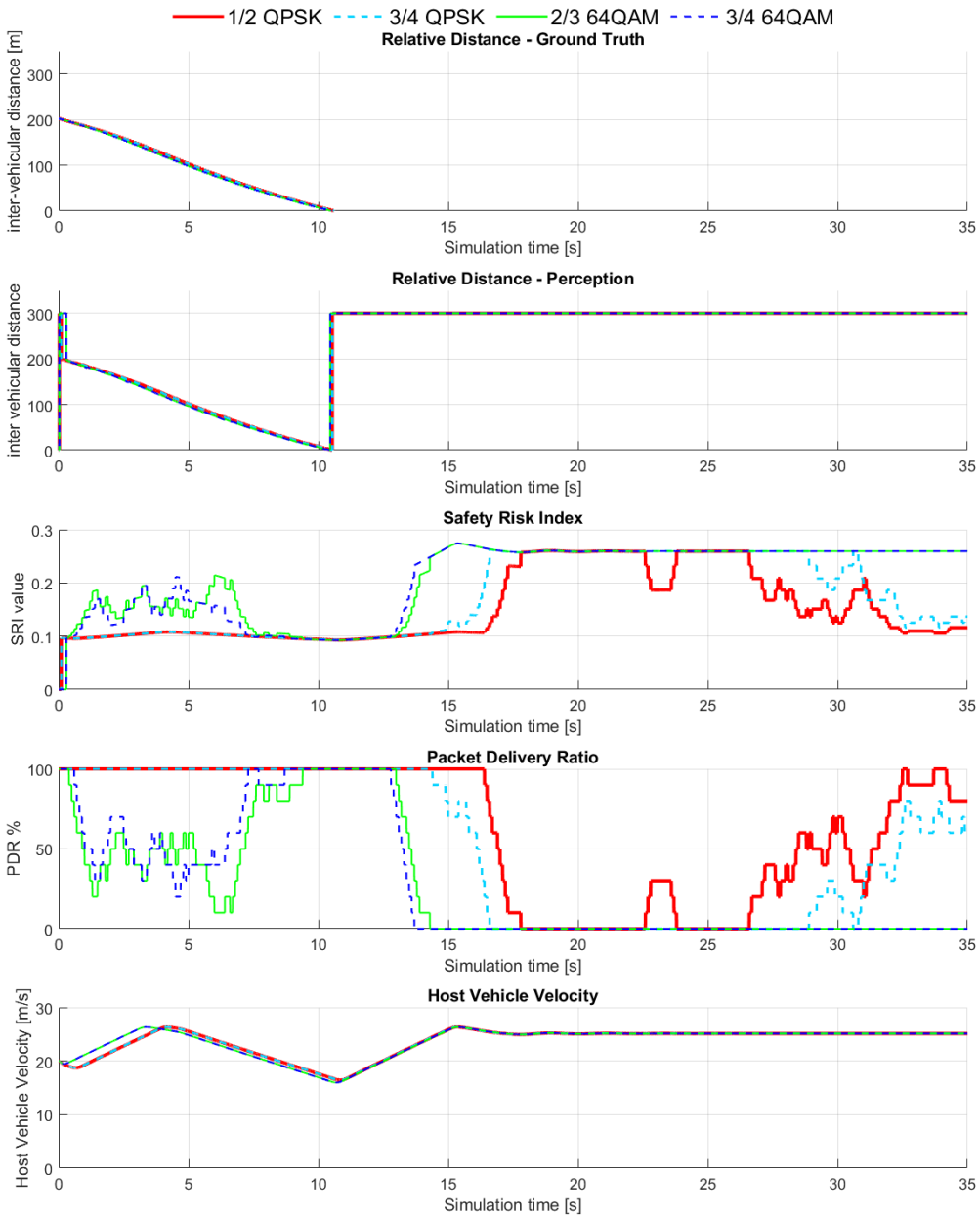

Figure 9. Results from simple CACC for high relative velocity (22.22 m/s = 80 km/h).

At last, we can assess the effectiveness of our proposed control in the context of a high delta velocity scenario. As previously observed, SRI was already above our target value at the beginning of the simulation due to the high velocities and the degraded network. Consequently, the control reduced the HV velocity to 10 m/s, as illustrated in Figure 10. With this method, we chose a more careful option, and the vehicle was able to adapt to the speed of the remote vehicle and keep a safe distance with each modulation.

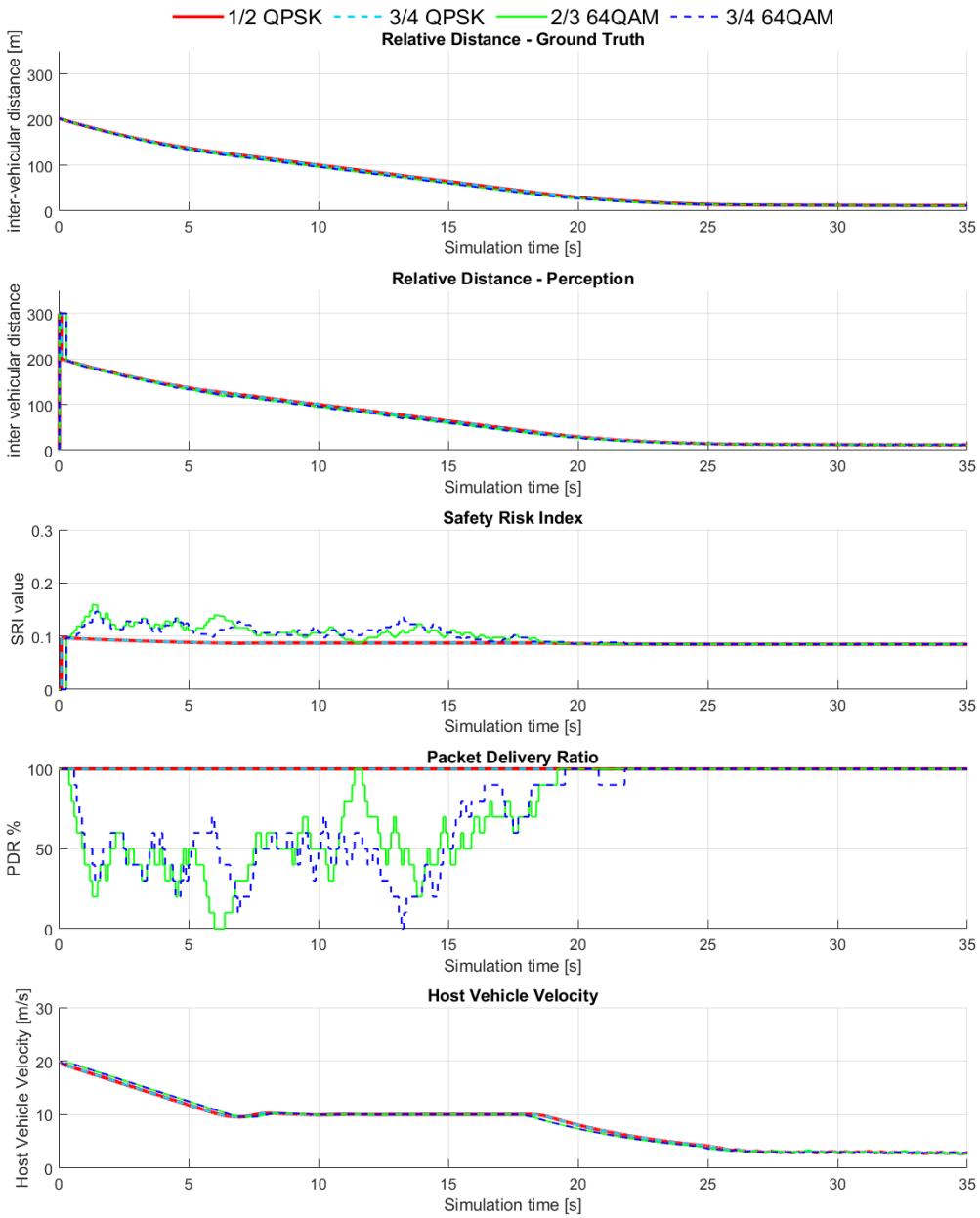

Figure 10. Results from SRI-based CACC for high relative velocity (22.22 m/s = 80 km/h).

4.4. Comparison

In order to better visualize the differences between the simple CACC and the proposed model, we created the following figures. In this section, we have chosen the high relative velocity scenario to compare as it could show relevant information for both controls.

In Figure 11, the different QPSK modulations can be seen with and without the proposed model. The continuous lines show the SRI-based CACC results. Due to the high relative velocity, the safety risk was high from the beginning even when the communication was good. The dashed lines show the simple method where the control could not stop the host vehicle in time. Following the collision, which occurred approximately 11 s into the simulation, the presented plots are no longer valid.

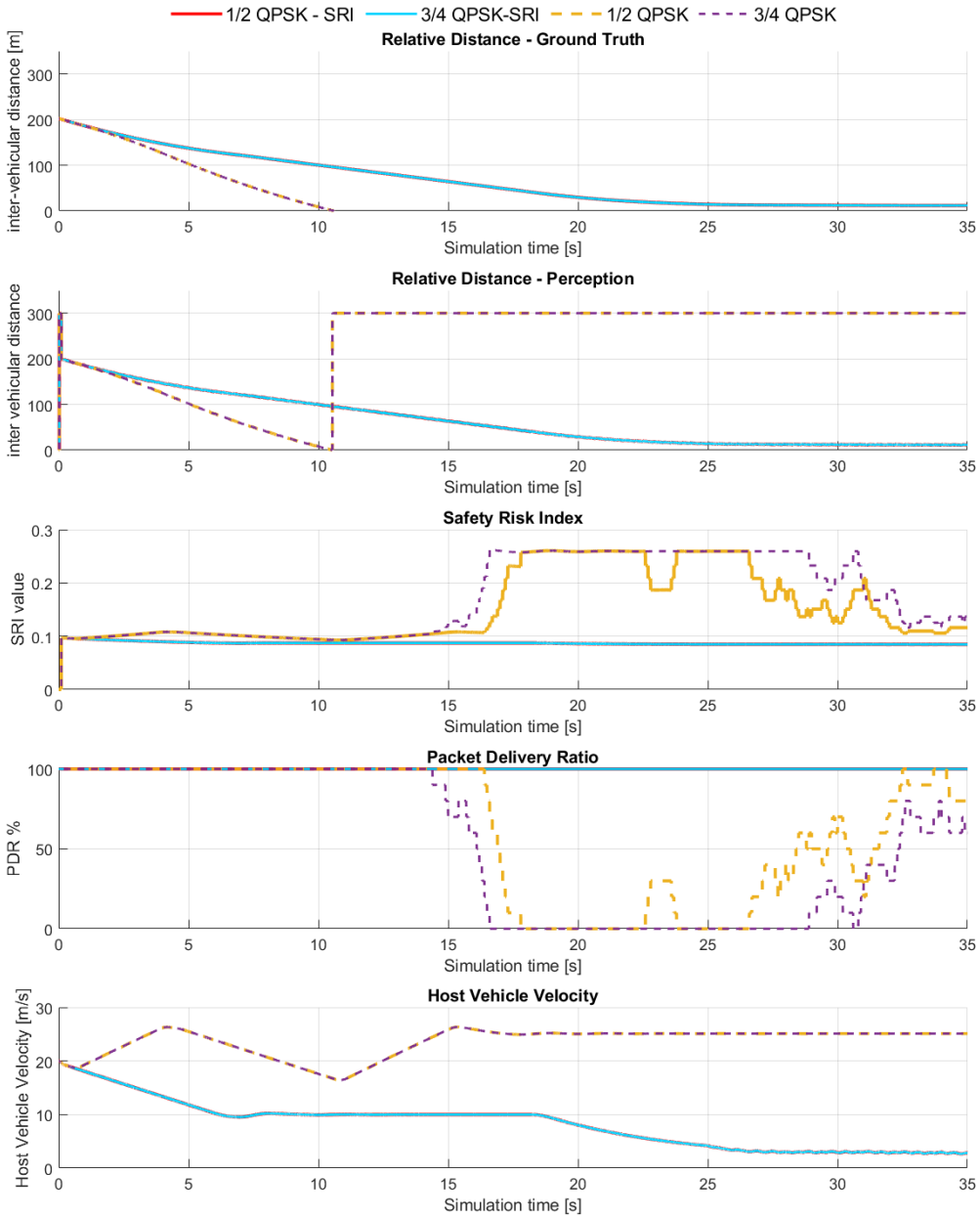

Figure 11. Results comparison for high relative velocity QPSK modulation (22.22 m/s = 80 km/h).

In Figure 12, comparisons of 64QAM modulations are presented. In this case, all of the modulations were affected by the noise. Here, the simple method could not stop the HV in time and collision with the RV occurred. Due to the high relative velocities and the degraded network, the proposed model started to decrease the HV velocity, and with this, the vehicle could adapt to the RV velocity. At around 20 s, the network started to get better even with the noise as the relative distance decreased.

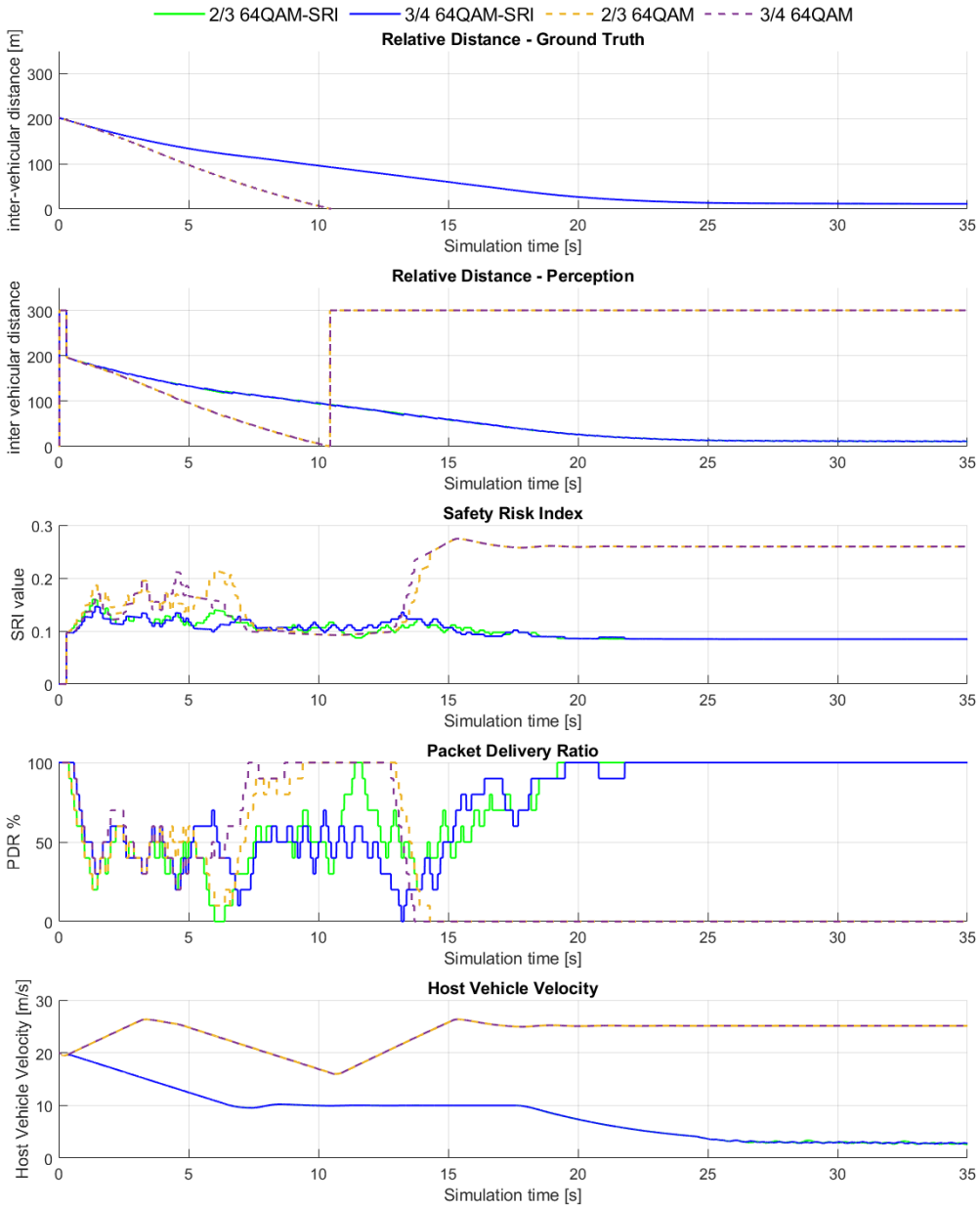

Figure 12. Results comparison for high relative velocity 64QAM modulation (22.22 m/s = 80 km/h).

4.5. Noise-Affected Zone

In our research, we investigated the noise effect on the communication and on our proposed control. For this, we created different scenarios mentioned in Section 3. In the executed tests, our HV and RV moved in a noisy field generated by a noise generator bacon at 400 m with a peak power of 20 dB.

In Figure 13, similar curves can be observed when there was no additional control involved. In the case of high relative velocity, at around 10 s, all modulations crashed with the RV. Moreover, when there was a moderate relative velocity, only the higher coding rate version of the 64QAM modulation resulted in a crash, which explains the split of curves.

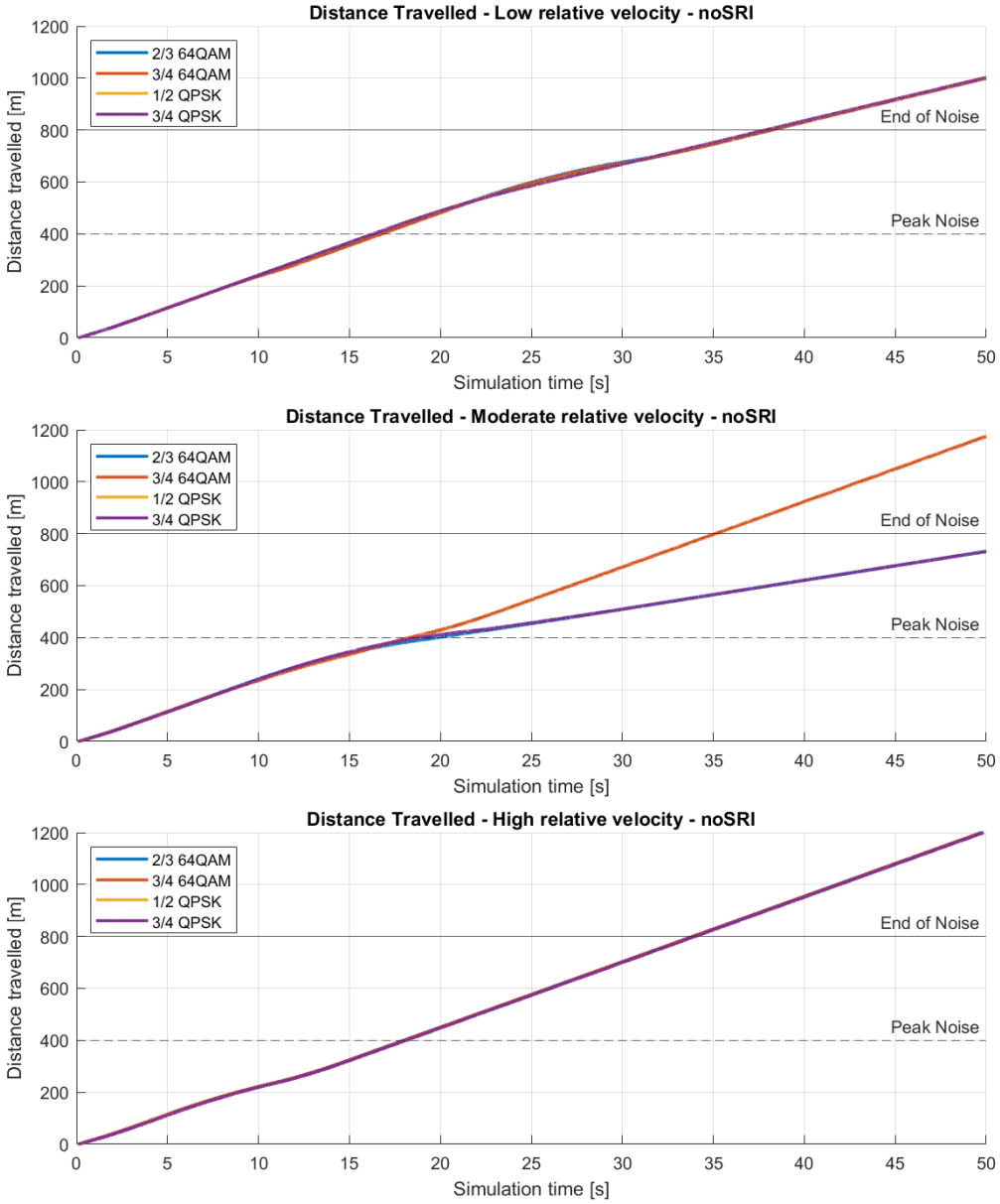

Figure 13. Distance traveled by HV without SRI in different scenarios.

Figure 14 shows the distance covered by the HV through the whole simulation of 50 s.

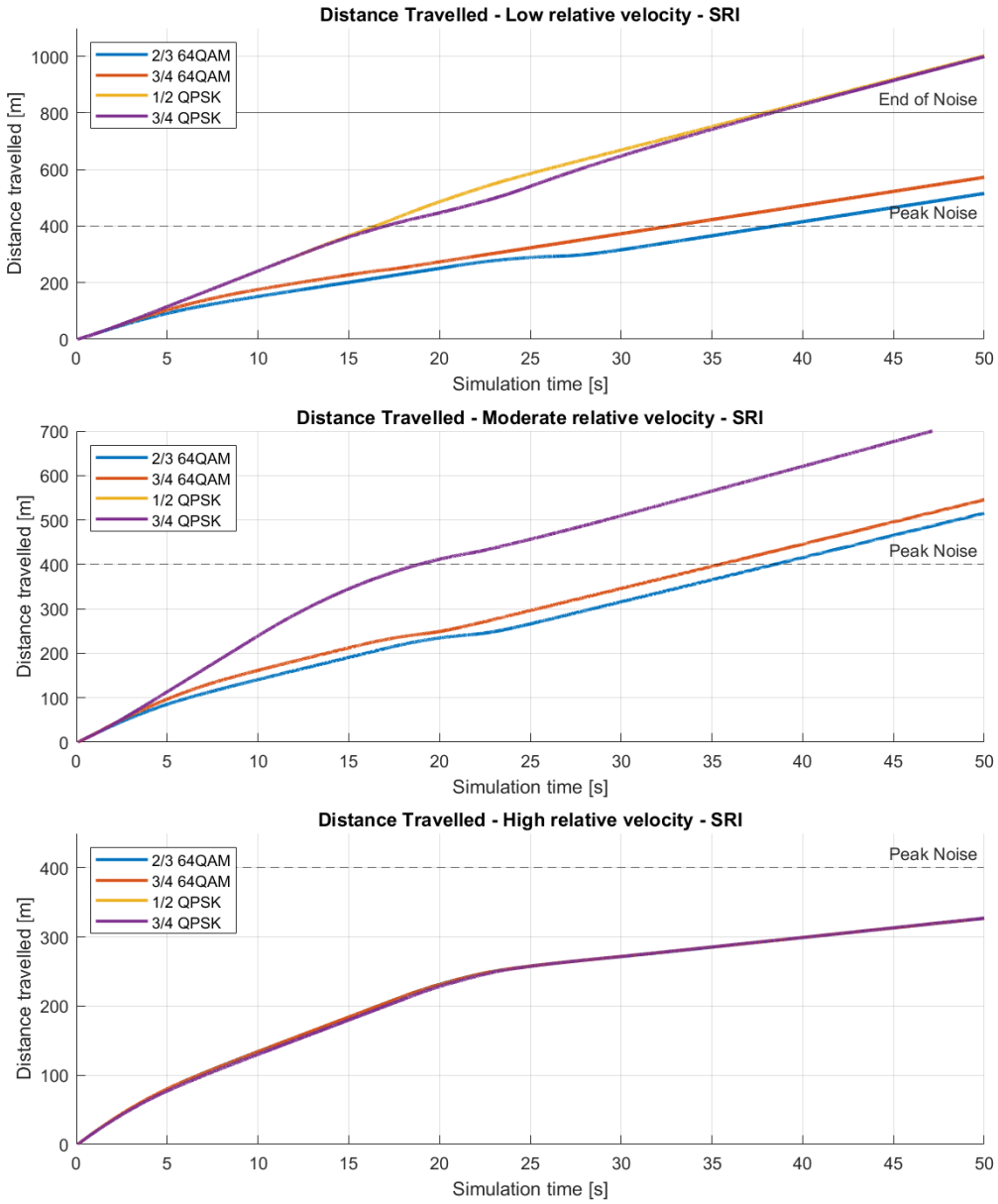

Figure 14. Distance traveled by HV with SRI in different scenarios.

4.6. Performance Evaluation

In order to evaluate our method, we proposed a simple evaluation to see how our concept is working. In our study, we evaluate our system from the perspective of safety. According to this, we have chosen the headway as our main parameter to see the performance of this solution.

$$Headway = \frac{relative\ distance}{v_{HV}}[\mathrm{s}] \tag{7}$$

Headway is defined as the fraction of the relative distance and the HV velocity (Equation (7)). For our research, we calculated the headway values for the whole scenario and introduced the Scenario Aggregate Headway (SAH) (Equation (8)).

$$SAH = \sum_{t} \frac{relative\ distance\ (t)}{v_{HV}\ (t)} \tag{8}$$

To provide a comparable performance metric, we calculated the sum of headway values with a sampling time (t) of 0.1 s for the whole scenario. In the case of negative relative distance, when collision occurred, we calculated with a zero value for the relative distance. To be able to create a safety performance indicator for our study, we have chosen a headway reference value of 1.5 s (Equation (9)).

$$SAH_{ref} = \sum_{t} 1.5 \tag{9}$$

Based on these equations, we could calculate the safety performance (SP) for our control by dividing SAH with the reference SAH in Equation (10).

$$SP = \frac{SAH}{SAH_{ref}} \tag{10}$$

In Table 4, we can see the different scenarios and different modulations' SP values. For a better evaluation of performance, we executed a couple more scenarios: one with a constant additional noise level of 10 dB and one with the same 400 m radius circle but with a lower noise peak power. Based on Table 4, we can see that values greater than 1 mean that there was no collision in that scenario. Without our proposed control concept, we can see that, in the case of high relative velocity, an accident occurred in all cases. With the introduction of our safety concept, higher values can be seen for the safety performance, which shows that our concept could be a good direction of development in the future. However, in some cases, the performance values are higher than what they should be, which shows that our concept is overcautious and needs further optimization.

Table 4. Safety performance (SP) evaluation of CACC.

Scenario	Modulations	Constant 10 dB Noise	400 m Radius with 10 dB Peak Noise	400 m Radius with 20 dB Peak Noise
Low relative velocity without SRI	1/2 QPSK	1.99	2.02	2.02
	3/4 QPSK	2.01	2.02	2.03
	2/3 64QAM	2.63	2.03	2.23
	3/4 64QAM	2.64	2.05	2.27
Moderate relative velocity without SRI	1/2 QPSK	1.84	1.85	1.85
	3/4 QPSK	1.83	1.85	1.85
	2/3 64QAM	2.12	1.85	1.95
	3/4 64QAM	2.11	2.20	1.36
High relative velocity without SRI	1/2 QPSK	0.91	0.98	0.98
	3/4 QPSK	0.91	0.98	0.98
	2/3 64QAM	0.88	0.92	0.91
	3/4 64QAM	0.88	0.92	0.91
Low relative velocity with SRI	1/2 QPSK	2.02	2.02	2.03
	3/4 QPSK	2.26	2.02	2.63
	2/3 64QAM	7.46	18.53	7.26
	3/4 64QAM	7.77	14.91	6.80
Moderate relative velocity with SRI	1/2 QPSK	1.93	1.84	1.84
	3/4 QPSK	3.19	1.84	1.84
	2/3 64QAM	2.34	14.24	8.65
	3/4 64QAM	2.33	8.50	8.67
High relative velocity with SRI	1/2 QPSK	3.58	3.66	3.66
	3/4 QPSK	3.59	3.66	3.66
	2/3 64QAM	0.84	3.34	3.58
	3/4 64QAM	0.83	3.10	3.59

5. Conclusions

In conclusion, we have identified several observations derived from the simulation and the results. Due to the inherent nature of the concept introduced, we can observe an inverse proportionality between the PDR and SRI values, which indicates that as the network begins to degrade and received packets begin to drop, the risk indicator will increase. Furthermore, we have demonstrated that our suggested control concept could provide a valuable foundation for future developments, as it can consider the severity of the situation within a degraded network. Despite the proposed control being safer and

not resulting in a collision in any of our scenarios, it was overly cautious when the relative velocities were low or medium. Moreover, when the communication network is down or very weak for an extended period, the controller must indicate this and return the control to the driver. Therefore, further development and calibration are necessary in future research to create an all-around solution.

In summary, we developed a simulation environment to simulate a V2X communication physical layer and to examine the impact of additional noise on network performance. For DSRC, we separated four different modulation types to enable the examination of the different modulations in a degraded network. Furthermore, we proposed a control concept and demonstrated that the improvement direction could be beneficial, although further developments and adjustments are required. It can be concluded that the proposed control mechanism is capable of warning the driver when the circumstances are worsening.

For future research, it would be beneficial to investigate this proposed model in greater depth. One possible avenue for further research would be to extend the simulation environment to enable the simulation of communication latency. This could lead to the development of a more complex and effective solution for the autonomous driving industry.

Author Contributions: Conceptualization, Z.P. and Á.T.; Methodology, Z.P., Á.T. and R.N.; Software, R.N.; Validation, Z.P., Á.T. and R.N.; Formal Analysis, Z.P., Á.T. and R.N.; Investigation, Z.P., Á.T. and R.N.; Resources, Z.P., Á.T. and R.N.; Writing—Original Draft Preparation, R.N.; Writing—Review and Editing, Á.T.; Visualization, R.N.; Supervision, Z.P. and Á.T.; Project Administration, Z.P. and Á.T.; Funding Acquisition, Z.P., Á.T. and R.N. All authors have read and agreed to the published version of the manuscript.

Funding: This research was supported by the European Union within the framework of the National Laboratory fo Autonomous Systems (RRF-2.3.1-21-2022-00002). Supported by the ÚNKP-23-4-I-BME-158 New National Excellence Program of the Ministry for Culture and Innovation from the source of the National Research, Development and Innovation Fund.

Institutional Review Board Statement: Not applicable.

Informed Consent Statement: Not applicable.

Data Availability Statement: The raw data supporting the conclusions of this article will be made available by the authors on request.

Conflicts of Interest: Author Roland Nagy was employed by the company Jaguar Land Rover Hungary Ltd. Organization. The remaining author declare that the research was conducted in the absence of any commercial or financial relationships that could be construed as a potential conflict of interest.

References

1. Moradi-Pari, E.; Tian, D.; Bahramgiri, M.; Rajab, S.; Bai, S. DSRC versus LTE-V2X: Empirical Performance Analysis of Direct Vehicular Communication Technologies. *IEEE Trans. Intell. Transp. Syst.* **2023**, *24*, 4889–4903. [CrossRef]
2. Bey, T.; Tewolde, G. Evaluation of DSRC and LTE for V2X. In Proceedings of the 2019 IEEE 9th Annual Computing and Communication Workshop and Conference (CCWC), Las Vegas, NV, USA, 7–9 January 2019; pp. 1032–1035.
3. Cui, L.; Hu, J.; Park, B.B.; Bujanovic, P. Development of a simulation platform for safety impact analysis considering vehicle dynamics, sensor errors, and communication latencies: Assessing cooperative adaptive cruise control under cyber attack. *Transp. Res. Part C Emerg. Technol.* **2018**, *97*, 1–22. [CrossRef]
4. Zhang, Y.; Zhang, J. Design and optimization of cluster-based DSRC and C-V2X hybrid routing. *Appl. Sci.* **2022**, *12*, 6782. [CrossRef]
5. Petrov, T.; Sevcik, L.; Pocta, P.; Dado, M. A performance benchmark for dedicated short-range communications and lte-based cellular-v2x in the context of vehicle-to-infrastructure communication and urban scenarios. *Sensors* **2021**, *21*, 5095. [CrossRef]
6. Maglogiannis, V.; Naudts, D.; Hadiwardoyo, S.; Van Den Akker, D.; Marquez-Barja, J.; Moerman, I. Experimental V2X evaluation for C-V2X and ITS-G5 technologies in a real-life highway environment. *IEEE Trans. Netw. Serv. Manag.* **2021**, *19*, 1521–1538. [CrossRef]
7. Karoui, M.; Freitas, A.; Chalhoub, G. Performance comparison between LTE-V2X and ITS-G5 under realistic urban scenarios. In Proceedings of the 2020 IEEE 91st Vehicular Technology Conference (VTC2020-Spring), Virtual, 25 May–31 July 2020; pp. 1–7.
8. Yang, A.; Weng, J.; Cheng, N.; Ni, J.; Lin, X.; Shen, X. DeQoS attack: Degrading quality of service in VANETs and its mitigation. *IEEE Trans. Veh. Technol.* **2019**, *68*, 4834–4845. [CrossRef]

9. Knowles Flanagan, S.; Tang, Z.; He, J.; Yusoff, I. Investigating and modeling of cooperative vehicle-to-vehicle safety stopping distance. *Future Internet* **2021**, *13*, 68. [CrossRef]
10. Schmidt, R.K.; Köllmer, T.; Leinmüller, T.; Böddeker, B.; Schäfer, G. Degradation of Transmission Range in VANETs caused by Interference. *PIK—Prax. Informationsverarbeitung Kommun.* **2009**, *32*, 224–234. [CrossRef]
11. Hoque, M.A.; Rios-Torres, J.; Arvin, R.; Khattak, A.; Ahmed, S. The extent of reliability for vehicle-to-vehicle communication in safety critical applications: An experimental study. *J. Intell. Transp. Syst.* **2020**, *24*, 264–278. [CrossRef]
12. Choi, J.; Kim, H. A QoS-aware congestion control scheme for C-V2X safety communications. In Proceedings of the 2020 IEEE Vehicular Networking Conference (VNC), Virtual, 16–18 December 2020; pp. 1–4.
13. Park, Y.J.; Sung, S.M.; Kim, J.Y.; Jung, J.I. Interference Rejection Combining Approach in Vehicle Communication Systems for Throughput Enhancement. *Electronics* **2021**, *10*, 1922. [CrossRef]
14. Ali, G.M.N.; Ayalew, B.; Vahidi, A.; Noor-A-Rahim, M. Feedbackless relaying for enhancing reliability of connected vehicles. *IEEE Trans. Veh. Technol.* **2020**, *69*, 4621–4634. [CrossRef]
15. Thunberg, J.; Bischoff, D.; Schiegg, F.A.; Meuser, T.; Vinel, A. Unreliable V2X communication in cooperative driving: Safety times for emergency braking. *IEEE Access* **2021**, *9*, 148024–148036. [CrossRef]
16. Liu, Y.; Wang, W. A safety reinforced cooperative adaptive cruise control strategy accounting for dynamic vehicle-to-vehicle communication failure. *Sensors* **2021**, *21*, 6158. [CrossRef] [PubMed]
17. Xue, S.; Gong, S.; Li, X. A Comparative Study of IEEE 802.11 bd and IEEE 802.11 p on the Data Dissemination Properties in Dynamic Traffic Scenarios. *Appl. Sci.* **2024**, *14*, 2099. [CrossRef]
18. Wippelhauser, A.; Edelmayer, A.; Bokor, L. A Declarative Application Framework for Evaluating Advanced V2X-Based ADAS Solutions. *Appl. Sci.* **2023**, *13*, 1392. [CrossRef]
19. Ibrahim, A.M.; Chen, Z.; Wang, Y.; Eljailany, H.A.; Ipaye, A.A. Optimizing V2X Communication: Spectrum Resource Allocation and Power Control Strategies for Next-Generation Wireless Technologies. *Appl. Sci.* **2024**, *14*, 531. [CrossRef]
20. Pethő, Z.; Szalay, Z.; Török, Á. Safety risk focused analysis of V2V communication especially considering cyberattack sensitive network performance and vehicle dynamics factors. *Veh. Commun.* **2022**, *37*, 100514. [CrossRef]
21. *ETSI EN 302 637-2 v1. 3.1*; Intelligent Transport Systems (Its); Vehicular Communications; Basic Set of Applications; Part 2: Specification of Cooperative Awareness Basic Service. ETSI: Sophia Antipolis, France, 2014.
22. Kryszkiewicz, P.; Sroka, P.; Sybis, M.; Kliks, A. Path loss and shadowing modeling for vehicle-to-vehicle communications in terrestrial TV band. *IEEE Trans. Antennas Propag.* **2022**, *71*, 984–998. [CrossRef]
23. Bazzi, A.; Masini, B.M.; Zanella, A. Cooperative awareness in the internet of vehicles for safety enhancement. *EAI Endorsed Trans. Internet Things* **2017**, *3*, e5. [CrossRef]
24. *IEEE 802.11-2012*; IEEE Standard for Information Technology–Telecommunications and Information Exchange between Systems Local and Metropolitan Area Networks–Specific Requirements Part 11: Wireless LAN Medium Access Control (MAC) and Physical Layer (PHY) Specifications. C/LAN/MAN—LAN/MAN Standards Committee: Washington, DC, USA, 2012; pp. 1–2793. [CrossRef]